Evaluation of Number Average Length Analysis in Quantifying Double Strand Breaks in Genomic DNAs†

Betsy M. Sutherland,*,‡ Paula V. Bennett,‡ Alexandros G. Georgakilas,‡ and John C. Sutherland‡,§

Department of Biology, Brookhaven National Laboratory, Building 463, 50 Bell Avenue, Upton, New York 11973-5000

Received August 23, 2002

ABSTRACT: Double strand breaks in DNA can be quantified down to very low frequencies (a few per Gigabase pair) in nanogram quantities of nonradioactive, genomic DNA by dispersing the DNAs on electrophoretic gels, digitizing them by quantitative electronic imaging, and calculating the DNA lengths by number average length analysis. No specific distribution of damages is required for number average length analysis. To test the validity of this approach, we used DNA populations of known absolute lengths and break frequencies as experimental DNAs and calculated the number average lengths and double strand break levels. Experimental DNAs and length standards were dispersed using pulsed field electrophoretic modes (unidirectional pulsed field, contour clamped homogeneous field, or transverse alternating field) appropriate for their size range, stained with ethidium, destained, and a quantitative electronic image obtained. A dispersion curve was constructed from the migration−mobility relationships of the length standard DNAs, and the number average lengths of the experimental DNAs were calculated. The calculated DNA lengths agreed well with the actual lengths. Furthermore, the double strand break frequencies calculated through number average length analysis of DNAs dispersed by these pulsed field gel modes and digitized by quantitative electronic imaging were in excellent agreement with the actual values for populations of DNA over the size range of ∼4 kbp to ∼3 Mbp. The use of this approach in quantifying DNA damages is illustrated for double strand breaks and damage clusters (e.g., OxyPurine clusters recognized by *Escherichia coli* Fpg protein) induced in T7 DNA by ionizing radiation.

Double strand breaks (DSBs)[1] are produced by damaging agents such as radiation or radiomimetic anti-cancer drugs and by normal cellular processes, for example, recombination. Measuring the level of DSBs and tracking their production and rejoining are key to understanding their roles and consequences. Many methods have been described for detecting, estimating, or quantifying DSB levels in genomic DNAs. Some of these methods provide qualitative indications of break levels, while others give quantitative measures of break frequencies.

Number average length analysis, based on the method of moments calculation of average lengths of DNA populations, is a standard among physical−chemical approaches for computing the average sizes of populations of macromolecules (*1*). It is a powerful and useful method because it does not require any specific distribution of damages. With the use of megabase-size DNAs and accurate, high sensitivity detection (*2*−*4*), it allows quantification of damages at levels as low as a few per gigabase pair (*5*).

It is useful to validate new approaches by comparison with simultaneous or previous data obtained on identical samples. We showed previously that number average length determination and methods of moments calculation of levels of single strand breaks (induced by enzymatic cleavage at pyrimidine dimer sites) from an electronic image of an electrophoretic gel containing ethidium-bromide stained human DNA from UV irradiated cells gave the same dimer levels as the same sample DNAs dispersed on alkaline sucrose gradients (*6*). We also developed electrophoretic gel-based methods for quantifying—on a damage per kbp or per Mbp or per Gbp basis—double strand breaks and bistranded DNA damage clusters (which are converted to de novo DSBs through cleavage at cluster sites) induced by very low doses of ionizing radiation (*5*, *7*, *8*). Ideally, data from such a method would be evaluated by comparison to results from other methods for quantifying radiation-induced DSBs at similar frequencies. However, most assay methods do not extend to damage levels obtained at very low radiation doses. Furthermore, some methods of damage detection yield empirical measures of damage levels (e.g., tail moments of the comet assay and the fraction of activity released of the FAR assay) that cannot be compared directly with absolute DSB frequencies. In addition, significantly different damage yields per unit dose are obtained from various methods that do measure DSB yields at higher doses and may reflect

† Supported by the Low Dose Program of the Office of Biological and Environmental Research of the US Department of Energy and by grants from the National Institutes of Health (R01 CA 86897 to B.M.S. and CA 88335 to J.C.S.).

* To whom correspondence should be addressed. E-mail: bms@bnl.gov. Phone: (631) 344-3380. Fax: (631) 344-3407.

‡ Biology Department.

§ Physics Department, East Carolina University, Greenville, NC 27858-4353.

[1] Abbreviations: CHEF, contour-clamped homogeneous field electrophoresis; DSB, double strand break; FAR, fraction of (radio)activity released; Gbp, gigabase pair (10^9 base pairs); kbp, kilobase pair; *L*, number average molecular length; Mbp, megabase pair; SSB, single strand break; TAFE, transverse alternating field electrophoresis; UPFE, unidirectional pulsed field electrophoresis.

10.1021/bi0205505 CCC: $25.00
Published on Web 03/04/2003

differences in experimental conditions as well (*9*, *10*).

We addressed the problem of lack of directly comparable previous methods by using systems in which the absolute break frequencies are known. These consist of DNA populations of known intact size in which the relative number and lengths of individual component molecules are also known and in which all fragments are present in equal numbers. The first system consists of restriction fragments of T7 bacteriophage and the intact 39.9 kbp T7 DNA molecule. The second systems consist of chromosomal DNAs of two yeast genomes (*Hansenula wingei* and *Saccharomyces cerevisiae*). In each case, the chromosomes can be considered fragments resulting from restriction of a virtually ligated supermolecule composed of all of that species' chromosomes that migrate into a gel. *H. wingei* chromosomes range from 1.05 to 3.13 Mbp, with a virtually ligated supermolecule length of 14.07 Mbp; *S. cerevisiae* chromosomes range from 225 kbp to 2.2 Mbp, with the length of a supermolecule containing all these chromosomes of 13.36 Mbp. We also tested *S. cerevisiae* chromosomes of the size range of ~1 Mbp, the range used to quantify DSBs in the NotI digest of human DNA (*5*). These systems can be used to test the accuracy of number average length analysis of break levels since the theory underlying this approach does not make any assumptions on the distribution of the breaks in DNA molecules.

We dispersed these DNAs by electrophoresis regimes appropriate for the DNA sizes to be separated: unidirectional pulsed field electrophoresis (UPFE) for molecules up to a few hundred kbp, transverse alternating field electrophoresis (TAFE) for those up to ~2 Mbp, and contour clamped homogeneous electric field (CHEF) for molecules to ~6 Mbp. Using dispersion curves obtained from the migration versus length relation of DNAs of known lengths, we then calculated the number average molecular length ($\bar{L}$) of individual molecular species in the populations. The calculated and expected lengths were in good agreement, verifying the correctness of the number average length calculations. Furthermore, the calculated break frequencies agreed with the actual frequencies for all the populations tested: for T7 and its restriction fragments, <40 kbp (1, 2, and 3 actual breaks vs 1.3, 2, and 2.8 calculated), for the *S. cerevisiae* chromosomal complement (14 actual breaks and 13.95 calculated), for the four *S. cerevisiae* chromosomes in the ~1 Mbp size range (3 actual breaks vs 2.9 calculated), and for the seven chromosomes of *H. wingei*, lengths ~1−3 Mbp (6 actual, 5.96 and 5.73 calculated). These data show that number average length analysis of gels using pulsing regimes appropriate for the DNA sizes to be separated, carried out with quantitative biochemical techniques and quantitative electronic imaging, provide excellent measures of the true double strand break frequencies in DNA molecules ranging in size from a few kbp to several Mbp.

We then used this approach to quantify ionizing radiation-induced complex damages containing multiple lesions on opposing strands within a few helical turns. One such damage is the double strand break, which can be regarded as (at least) two single strand breaks (SSBs) on opposing DNA strands within a few helical turns. However, DSBs comprise only ~20−30% of the complex damages in DNA irradiated in solution or in human cells; clusters of oxidized purines, oxidized pyrimidines, or abasic sites constitute the majority of such multi-lesion damages (*7*, *11*, *12*). We show here the application of number average length analysis to quantitation of DSBs and OxyPurine clusters (recognized by *Escherichia coli* Fpg protein) and compare these results with previous data.

THEORY

The theory underlying quantitation of DNA damage from the average lengths of heterogeneous DNA populations can be applied to DNA separated by centrifugation or gel electrophoresis (*4*, *6*, *13*) and has recently been extended to single molecule sizing (*14*). For both centrifugation and electrophoresis, the analysis is complicated by the nonlinear relationship between the size of DNA molecules and the speed with which they move under the influence of a centripetal or electrical force.

Strand Break Quantitation by Number Average Length Analysis. Consider a population of N duplex DNA molecules in which the ith molecule contains L_i base pairs. The average length of the molecules in the population is given by the expression in eq 1. Formally, this is called the number average length of the molecules in the population to distinguish it from certain other types of averages that are used to describe the distribution of lengths in a population of polymers (*1*). The summation in the numerator of the expression on the right-hand side of eq 1 is just the total number of base pairs in the sample. The U subscripts indicate that this is an initial or untreated sample, in contrast to the sample described below.

$$\bar{L}_{\mathrm{U}} = \frac{\sum_{i=1}^{N} L_{\mathrm{i}}}{N_{\mathrm{U}}} \tag{1}$$

Suppose that the sample is treated to introduce M double strand breaks into the population of the original N_{U} molecules. These breaks could be randomly distributed, could be produced at specific sites in the molecules, or could have many other distributions. Double strand breaks produced by ionizing radiation are, to some approximation, randomly distributed, while the strand breaks produced by restriction endonucleases are located at specific sites. Regardless of the distribution, each strand break results in the formation of two (smaller) molecules for each molecule that existed before the break occurred. Thus, the number of molecules in the treated population, N_{T}, consists of $N_{\mathrm{U}} + M$ molecules, and the average length of the molecules in this population is shown in eq 2, where the T subscript indicates that this is a treated sample.

$$\bar{L}_{\mathrm{T}} = \frac{\sum_{i=1}^{N_{\mathrm{U}}+M} L_{\mathrm{i}}}{N_{\mathrm{U}} + M} \tag{2}$$

The number of molecules is increased by the induction of strand breaks, but the number of base pairs is unchanged. Thus, the summation in the numerator of eq 2 is equal to the corresponding expression in eq 1, and both can be replaced by N_{bp}, the number of base pairs in the population.

Rearranging the equation $N_T = N_U + M$ gives $M = N_T - N_U$. Dividing by N_{bp} gives the frequency of breaks, Φ, as shown in eq 3.

$$\Phi = \frac{M}{N_{bp}} = \frac{N_T}{N_{bp}} - \frac{N_U}{N_{bp}} \quad (3)$$

Substituting N_{bp} for the summation in eqs 1 and 2, we obtain $\bar{L}_U = N_{bp}/N_U$ and $\bar{L}_T = N_{bp}/N_T$. Substituting these expressions into eq 3 results in the expression for Φ shown in eq 4.

$$\Phi = \frac{1}{\bar{L}_T} = \frac{1}{\bar{L}_U} \quad (4)$$

If the lengths of the molecules in the population are measured in base pairs, then Φ is the probability of a strand break per base pair. However, the lengths of the DNA molecules in the population can also be specified in some larger unit, such as kilobase pairs (kbp), megabase pairs (Mbp), or gigabase pairs (Gbp), in which case, Φ is the number of breaks per kbp, Mbp, or Gbp. In this case, Φ can be described as the frequency of breaks induced by the treatment. Thus, we can determine the frequency (in units such as breaks/Mbp) or probability per base pair of producing a double strand break by measuring the average length of the molecules in a population before and after some treatment or combination of treatments that produces strand breaks.

The average length of the molecules in a population can be obtained by measuring the average length of the molecules in a representative sample because both the numerator and the denominator of eq 1 and eq 2 scale as the mass of the DNA sample. That is, we need not examine all of the molecules in a population but only the molecules in a representative sample derived from that population. It follows that the determination of average lengths is insensitive to the mass of the sample chosen [as long as the DNA concentration is sufficiently low that individual molecules migrate as a function of their lengths (*15*)], so small differences in the DNA mass have no significant effect on the determination of the frequency of breaks.

Determining Number Average Lengths by Gel Electrophoresis. Suppose that a sample is separated by gel electrophoresis, and the DNA molecules are labeled with a fluorochrome such that the number of labels is proportional to the number of base pairs in the molecule but independent of base composition (the AT/GC ratio) and base sequence. Let $f(x)$ represent the fluorescence profile of a lane (above background) as a function of the distance of migration x through the gel. The total fluorescence originating from a small rectangular area centered a distance x from the well and with size determined by the width of the lane and an incremental length along the direction of migration Δx is equal to $f(x)\,\Delta x$. This product is proportional to the total number of DNA base pairs in the rectangular area. The total number of base pairs in the entire lane is proportional to the integral of this product over the length of the lane. (Note that we switch from the sums used above to integrals because the distance of migration, x, is a continuous variable.)

Suppose that $L(x)$ represents the contour length, measured in base pairs, of the DNA molecules migrating to position x during electrophoresis. While DNA length expressed in units of base pairs is always an integer, as was presumed in eqs 1 and 2, hereafter, we will treat $L(x)$ as a continuous function. Because the number of base pairs in most of the molecules in our samples is very large, this introduces no significant error. The number of DNA molecules in the small rectangle described above is thus proportional to the total number of base pairs divided by the number of base pairs per molecule [i.e., $f(x)\Delta x/L(x)$], and the proportionality constant is identical to that for the expression giving the number of base pairs, described above. Integrating the expression for the total number of molecules in each segment over the length of the gel gives the total number of DNA molecules in the lane. Thus, if we measure $f(x)$ and determine $L(x)$, we can compute the number average length of the molecules in the lane according to eq 5, which is obtained by substituting the integrals described above for the corresponding terms in eqs 1 and 2.

$$\bar{L} = \frac{\int f(x)\mathrm{d}x}{\int \frac{f(x)}{L(x)}\mathrm{d}x} \quad (5)$$

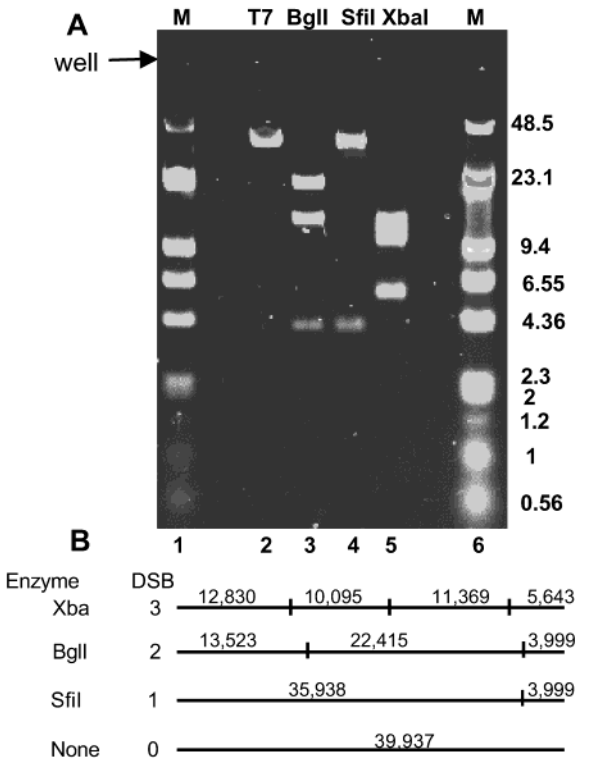

FIGURE 1: (A) Electronic image of unidirectional pulsed field electrophoretic gel containing T7 DNA (lane 2), BglI- (lane 3), SfiI- (lane 4), and XbaI- (lane 5) digests of T7, as well as molecular length standard DNAs [lanes 1 and 6, bacteriophage λ (48.5 kbp), HindIII digested λ (23.1, 9.4, 6.5, 4.4, 2.3, 2, and 0.56 kbp), and a 100 bp ladder]. (B) Diagram of restriction sites and fragment lengths for digestion of T7 DNA by XbaI (three sites), BglI (two sites), SfiI (one site), as compared to full-length T7 DNA.

EXPERIMENTAL PROCEDURES

Unidirectional Pulsed Field Electrophoresis. T7 DNA was digested with SfiI, BglI, or XbaI (New England BioLabs, Beverly, MA) according to the manufacturer's recommendations, producing the fragments shown in Figure 1. Reactions

were terminated by the addition of 100 mM EDTA, pH 8, to a final concentration of 15 mM. Intact T7 and restriction digests, along with double-stranded DNA length standards [bacteriophage λ (48.5 kbp), HindIII digested λ (23.1, 9.4, 6.5, 4.4, 2.3, 2, and 0.56 kbp), and a 100 bp ladder (2, 1.5, 1.2, 1, and 0.5 kbp; New England BioLabs)] were electrophoresed in 0.7 or 1% agarose, in Tris-acetate buffer, pH 8, using unidirectional pulsed field electrophoresis [UPFE, 15 V/cm; 0.3-s pulse, 10-s interpulse period, 16 h, 7 °C with buffer recirculation (*16*)]. Gels were stained with ethidium bromide (1 μg/mL) and destained, and a quantitative electronic image was obtained. A DNA dispersion curve was determined using the length standards. From the profiles of restriction enzyme-treated or untreated DNA populations, the number average length ($\bar{L}$) of each DNA distribution was calculated according to eq 5. From these number average lengths, the Φ_{DSB} (DSB frequency) was calculated according to eq 4.

Contour Clamped Homogeneous Electrophoretic Field (CHEF). Yeast chromosomal DNAs (*Schizosaccharomyces pombe*, *H. wingei*, and *S. cerevisiae*, all from BioRad, Hercules CA) were electrophoresed in either of two modes, as follows. Mode 1: 0.8% Sea Kem Gold agarose (Bio-Whittaker Molecular Applications, Rockland ME) in 0.5X TEB (1X TBE is 90 mM Tris borate, 2 mM EDTA, pH 7.8) in a BioRad CHEF DRII for 10 h using 0.5X TEB as electrophoresis buffer and a linearly ramping pulsing regime from 200 to 3600 s, at 70 V and 9 °C; the agarose plugs were then removed from the wells, and electrophoresis continued at 9 °C for 72 h using a linearly ramping pulsing regime from 3400 to 50 s, using a voltage of 65 V for 24 h, then 75 V for 24 h, followed by 80 V for 12 h and finally 85 V for 12 h. Mode 2: BioRad CHEF DRII, FMC Fastlane agarose, 0.5X TBE, pH 8.02, 60 s switching, 190 V, 15 h at 12 °C. Gels were stained with ethidium bromide (1 μg/mL) and destained, and an electronic image was obtained as described above. The DNA dispersion curve was determined from an analytical mobility function based on either the *S. pombe* and *S. cerevisiae* chromosome length standards, or these DNAs plus *H. wingei* chromosomes (Mode 1), or the *S. cerevisiae* chromosomes and λ ladders (Mode 2). The number average lengths of individual *H. wingei* chromosomes or of the entire *H. wingei* distribution were also calculated by eq 5. By considering the entire population of chromosomes to be the treated population, and the virtually ligated supermolecule comprised of the total of the lengths of the *H. wingei* chromosomes as the untreated population, the number of double-stranded scissions of the genomic molecule required to divide it into seven chromosomes was computed by eq 4.

Transverse Alternating Field Electrophoresis (TAFE). DNAs (*S. cerevisiae* chromosomes, λ ladders, both from BioRad) were electrophoresed using neutral transverse alternating field electrophoresis (TAFE (*17*), Gene Line I, Beckman, Fullterton, CA); 30 min at 90 V with a 4-s switching time, then 16 h at 190 V with a 60-s switching time; electrophoresis buffer, 10 mM Tris acetate, 0.5 mM EDTA (*5*). Gels were stained with ethidium bromide (1 μg/mL) and destained, and an electronic image was obtained as described above. The DNA dispersion curve was determined using an analytical mobility function, and the number average length of each *S. cerevisiae* chromosome was calculated according to eq 5. In addition, the number average length of the entire population of chromosomes was also calculated by eq 5. The number of double-stranded scissions of the genome required to divide it into the 15 chromosomes was then computed by eq 4; the entire population of *S. cerevisiae* chromosomes was considered to be the treated population, and the virtually ligated supermolecule of the total of the *S. cerevisiae* chromosomes on the gel was considered as the untreated population.

Radiation-Induced Double Strand Breaks and Oxidized Purine Clusters in T7 DNA. T7 DNA at 50 μg/mL in 20 mM KPO_4 in plastic tubes on ice was irradiated with ^{137}Cs γ-rays at a rate of 2.1 Gy/min or 50 kVp X-rays from a Picker Nuclear X-ray machine. Irradiations with γ-rays were carried out at the Brookhaven Controlled Environment Radiation Facility; irradiations and dosimetry were performed by a certified operator of the facility.

DNAs were equilibrated with 70 mM HEPES/KOH, pH 7.6, 100 mM KCl, 1 mM EDTA, 1 mM DTT, and 100 ng/μL bovine serum albumin, then treated with sufficient quantities of homogeneous Fpg protein to cleave at all cluster sites for that enzyme. For reactions containing 500 ng of T7 DNA, this corresponded to 60 ng of Fpg protein. Companion samples for determination of radiation-induced DSBs were incubated without enzyme. The nonspecific nicking of the enzyme preparation was evaluated by treatment of unirradiated supercoiled DNA at increasing enzyme, DNA ratios, and was found to be negligible for the preparations used in this report. Substrates for Fpg protein include 4,6-diamino-5-formamidopyrimidine (FapyAde) and 2,6-diamino-5-formamidopyrimidine (FapyGua), 2,6-diamino-4-hydroxy-5-*N*-methylformamidopyrimidine (MethylFapyGua), 8-oxo-7,8-dihydro-2′-deoxyguanosine (8-oxodGuo), some abasic sites, C8-oxoadenine, and to a lesser extent, other modified purines (*18*−*22*). Fpg protein has been reported to cleave some pyrimidine derivatives as single lesions in synthetic oligonucleotides but fails to release the same bases in DNA exposed to ionizing radiation (*19*, *23*, *24*). 5-Hydroxycytosine and 5-hydroxy-2′-deoxyuridine are substrates for Fpg protein, but neither is formed at significant levels during aerobic irradiations.

After digestion was complete, traces of Fpg protein were removed by addition of Proteinase K and EDTA to final concentrations of 1.33 mg/mL and 0.1 M, respectively, and incubation at 37 °C overnight. A neutral stop mixture (0.125% bromphenol blue, 0.5% sodium lauryl sulfate in 50% glycerol) was then added to ensure dissociation of any persistent DNA−protein complexes.

Damage Cluster Measurement. Samples were electrophoresed along with molecular length standards (DNA from bacteriophages λ and a HindIII digest of λ) in 0.4% agarose and Tris-acetate buffer, pH 8, using static field electrophoresis (30 V, 6 °C, with buffer recirculation) for cluster frequencies $>\sim$30 sites/Mbp or unidirectional pulsed field electrophoresis (*16*) (15 V/cm; 0.3-s pulse, 10-s interpulse, 16 h, 10 °C with buffer recirculation) for lower cluster frequencies. Multiple length standard lanes are used to allow precise alignment of the gel for imaging. Gels were stained, destained, and imaged as described above. The number average lengths were calculated according to eq 5. From these $\bar{L}$ values, the frequencies of DSBs, f_{DSB}, was calculated

from the following equation (*6*):

$$\phi_{DSB} = 1/\bar{L}(+\text{rad}) - 1/\bar{L}(-\text{rad}) \quad (6)$$

where $1/\bar{L}(+\text{rad})$ and $1/\bar{L}(-\text{rad})$ are the reciprocals of the number average lengths of irradiated and unirradiated samples. The frequencies of other cluster sites, f_C (determined by treatment of samples subjected to dose D, then subdivided; part was digested with Fpg protein, while the companion part was incubated without enzyme), were calculated from the equation

$$\phi_C = 1/\bar{L}(+\text{rad}_D, +\text{enzyme}) - 1/\bar{L}(+\text{rad}_D, -\text{enzyme}) \quad (7)$$

where $1/\bar{L}(+\text{rad}_D, +\text{enzyme})$ and $1/\bar{L}(+\text{rad}_D, -\text{enzyme})$ are reciprocals of number average lengths of sample pairs irradiated with dose D, with and without enzyme, respectively (*25*).

Hazardous Procedures. Pulsed field electrophoresis employs electrical fields, and precautions should be taken to observe the safe use of the apparatus. Ethidium bromide is a mutagen and must be handled and disposed of by appropriate means. Ultraviolet light in the transilluminator for gel imaging is a potential skin and eye hazard, and UV−opaque glasses with side shields and skin protection should be used.

RESULTS

Unidirectional pulsed field electrophoresis resolves molecules in the range of a few kbp to about a hundred kbp and requires a simple electrophoretic apparatus (*16*). Figure 1 shows an electronic image of an UPFE gel containing DNA length standards (M, lanes 1 and 6), full-length T7 DNA (39 937 bp), and fragments of T7 resulting from complete digestion with XbaI, BglI, or SfiI, as shown schematically below the gel image. Full-length T7 DNA provides an untreated population of DNA molecules, and the restriction fragments comprise treated populations containing DNA molecules whose lengths are known (since the sequence is known) and known numbers of restriction sites, scission at which produces a double strand break. These fragments provide test populations of known absolute DNA sizes and break frequencies.

In number average length analysis, the positions of migration and lengths of size-standard, double stranded, linear DNAs are used to construct a dispersion curve (Figures 2−4) (*4*, *6*, *16*). Using the UPFE dispersion curve of Figure 2, we calculated the number average lengths of the individual restriction fragments in the three digests. Figure 2 shows an example of such an analysis for BglI-restricted T7 DNA. The bars under individual peaks show the portion of the DNA profile used to calculate the number average length of each fragment. For the BglI digest, the number average lengths of the three fragments from three independent gels were calculated to be 21.65 ± 0.07, 14 ± 0.28, and 4.21 ± 0.83 kbp, in reasonable agreement with the actual lengths of 22.5, 13.5, and 4 kbp. As shown in Figures 2 and 5, similar analyses for the other restriction digests (lanes 4 and 5 of Figure 1) and for intact T7 DNA (lane 2) showed good agreement between the calculated and the actual lengths of these DNAs, in the range of ∼4−40 kbp. This correspondence of experimental number average lengths and actual DNA sizes indicates that the DNA separations,

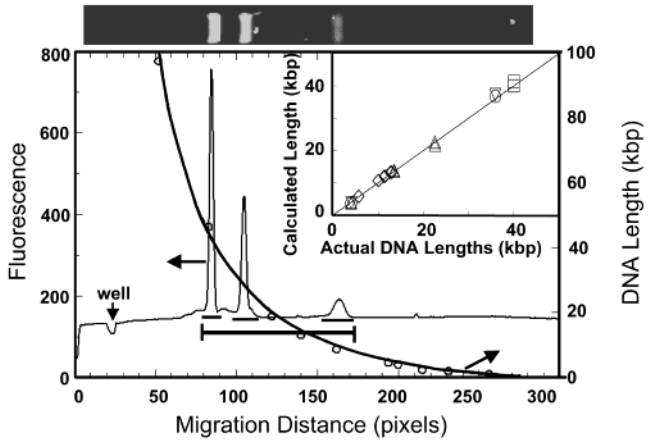

FIGURE 2: Unidirectional pulsed field gel profile of DNA fluorescence from BglI restriction of T7 DNA (left axis) and the calculated dispersion curve (right axis). The length standard DNAs (λ, 48.5 kbp; HindIII digest of λ (23.1, 9.4, 6.5, 4.4, 2.3, 2, and 0.56 kbp) and 100 bp ladder (2, 1.2, 1, and 0.5 kbp) are plotted on the dispersion curve (○). An electronic image of the gel lane containing Bg1I DNA is shown in register at the top of the plot. The portions of the profile used to analyze the lengths of the three fragments are shown by the lines beneath the profiles, and that used to analyze the number of breaks required to give the number average length of the entire population is shown by the heavy bar underlying all three peaks. The inset compares the calculated lengths of the restriction fragments from BglI (△), SfiI (▽), and XbaI (◊) cleavage and intact T7 (□) with the actual lengths known from the T7 sequence (*26*) and restriction site sequences for these enzymes. The solid line represents the ideal identity condition in which actual and experimental lengths are exactly equal.

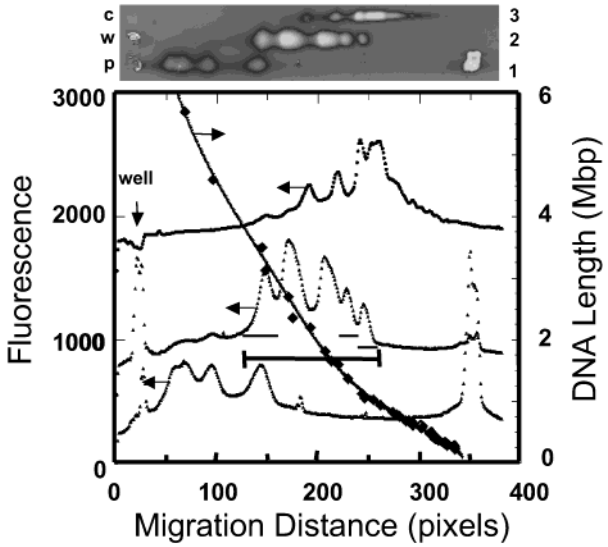

FIGURE 3: Contour clamped homogeneous field gel (Mode 1) fluorescence profiles of chromosomal DNAs of *S. pombe* (lower), *H. wingei* (middle), and *S. cerevisiae* (upper) (all left axis). The dispersion curve is shown as a smooth curve (right axis) with the yeast chromosomes used in its construction as data points (♦). T7 DNA is also present in the lower trace but was not used in construction of the dispersion curve. An electronic image of the lanes containing these DNAs is shown in register at the top of the figure. The lines under three *H. wingei* chromosomes show the portion of the profile used to calculate the $\bar{L}$ values of these three chromosomes. The heavy bar shows the portion of the profile used to calculate the number of breaks required to produce the seven *H. wingei* chromosomes from the virtually ligated supergenomic molecule.

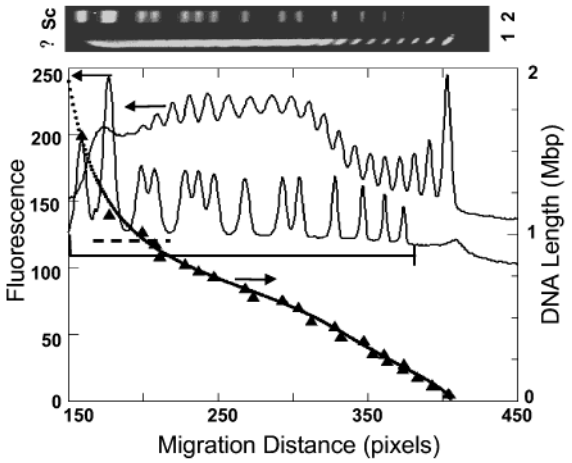

FIGURE 4: Transverse alternating field gel fluorescence profiles of λ ladders (upper) and chromosomes of *S. cerevisiae* (lower) (left axis) as well as the calculated dispersion curve (right axis). The DNAs used to calculate the dispersion curve (λ ladders and *S. cerevisiae* chromosomes) are shown as data points (▲). An electronic image of gel lanes containing these DNAs is shown above the figure (lane 1, λ multimers; lane 2, *S. cerevisiae* chromosomes). The heavy bar shows the portion of the profile used to calculate the number of breaks required to produce the 15 *S. cerevisiae* chromosomes from the virtually ligated supergenomic molecule.

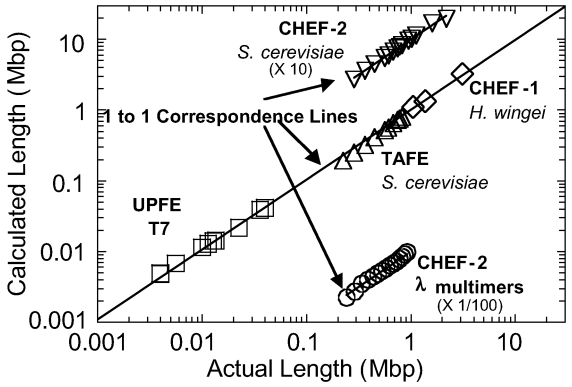

FIGURE 5: Calculated vs actual lengths for restriction digest fragments of T7 dispersed by UPFE (□), chromosomes of *S. cerevisiae* electrophoresed by TAFE (△), and *H. wingei* chromosomes separated using CHEF Mode 1 (◊). For clarity, the values for *S. cerevisiae* separated by CHEF Mode 2 are multiplied by 10 (▽), and those for λ multimers dispersed by CHEF-2 are divided by 100 (○). The lines represent the one-to-one correspondence lines for the calculated and actual values.

measurement of DNA masses, establishment of the dispersion curve, and $\bar{L}$ calculation were carried out correctly.

The key measure, however, for DNA damage quantitation is the DSB (in this case, restriction site) level in each of the three restricted (treated) DNA populations relative to the intact (untreated) T7 DNA molecule. The heavy bar in Figure 2 shows the portion of the DNA profile encompassing all three bands of the BglI digest that was used in number average length analysis, resulting in an average length of 13.40 kbp, which agrees well with the theoretical value of 13.312, obtained by dividing 39.937 [the actual length of T7 DNA (*26*)] by three. The calculated average length of the intact, uncleaved T7 molecule was 39.97 kbp, very close to the actual value. According to eq 2, the inverse of the length of the intact (using the calculated average length) T7 molecule (0.025018) is subtracted from the inverse of the average length of 13.405 kbp (0.074599) producing 0.0496

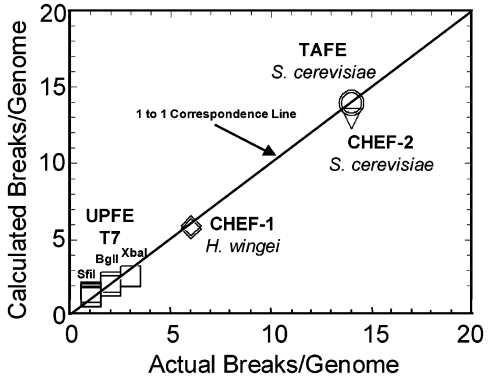

FIGURE 6: Calculated vs actual number of breaks required to give the number of fragments from the intact DNA T7 restriction fragments separated using UPFE (□), or to obtain the number of *H. wingei* chromosomes (separation by CHEF Mode 2, ▽), or to give the number of *S. cerevisiae* chromosomes from the virtually ligated supergenomic molecule (electrophoresis by TAFE (○, two independent determinations) or by CHEF Mode 1 (◊). The line shows the one-to-one correspondence lines for the calculated and actual values.

breaks/kbp. Using the calculated length of 39.972 kbp per T7 molecule, the product of the yield times the length (0.0496 × 39.972) is the frequency of breaks (restriction sites) per T7 molecule, or 1.98, in excellent agreement with the known number of two BglI sites per full-length T7 DNA. Data from three independent gels and analyses gave a frequency of 2.13 ± 0.14 sites/T7 molecule.

We also calculated the break frequency in SfiI- (contains one restriction site/T7 molecule) and XbaI- (contains three sites/T7) restricted T7 DNA populations. Figure 6 (squares) shows that the calculated and expected break frequencies in the three restriction digest populations agree well. Such agreement indicates that this method—including gel electrophoresis, ethidium staining, destaining, electronic imaging, calculation of the dispersion curve, and number average length determination by the methods of moments—provides accurate measures of the break frequency in molecules in the range of 4−40 kbp.

Number Average Length Analysis of Megabase Pair Length Chromosomal DNAs. Chromosomal DNAs of several yeast species also comprise molecules of known sizes that can be considered as members of a treated population, and their sum can be regarded as the size of an untreated molecule, a virtually ligated supermolecule. This provides DNAs—the individual chromosomes—of known sizes that provide a set of absolute length standards to use in constructing dispersion curves, checking the relation of the calculated number average length versus the known chromosome sizes, and in calculating the levels of breaks of the virtually ligated supermolecule required to generate the known number of chromosomes for each species.

Yeast chromosomal DNAs are too large to be resolved by either static field or unidirectional pulsed field electrophoresis. Contour-clamped electric field gel electrophoresis (CHEF) disperses DNAs in the range of a few kbp to several megabase pairs (*27*), and specific CHEF electrophoresis conditions can be used to resolve chromosomal DNAs in different size classes. Figure 3 shows an electronic image of a CHEF gel (electrophoresis Mode 1) containing chromosomal DNAs of *S. pombe* (lane 1, p), *H. wingei* (lane 2, w), and *S. cerevisiae* (lane 3, c), as well as the corresponding

DNA profiles from these lanes. The figure also shows the dispersion curve calculated from the length versus distance coordinates for each chromosome.

We focused on the *H. wingei* chromosomes since they are in the middle of the size range of DNA lengths dispersed by this CHEF regime; thus, all the chromosomes are well within the range of the high and low molecular length ends of the dispersion curve. They allow us to test first, whether the lengths of the partially resolved chromosomes can be accurately determined by average length analysis of the individual bands, and second, if average length analysis of the entire distribution correctly calculates the number of breaks of the virtually ligated supermolecule required to produce the seven chromosomes of *H. wingei*, even though they consist of overlapping bands (as would be found in a heterogeneous population of DNAs broken by ionizing radiation treatment).

Because of practical difficulties in determining the left and right edges of the poorly resolved 2.7 and 2.35 Mbp chromosomes and the 1.81 and 1.66 Mbp chromosomes, we analyzed three other chromosomes for which the limits of the DNA profile could be estimated more easily. The bars below these three peaks in Figure 3 show the portion of the profile used for analysis of the length of each fragment. Number average length analysis of the individual peaks yielded lengths of 3.42, 1.36, and 1.12 Mbp, in reasonable agreement with the expected lengths of 3.13, 1.37, and 1.05 Mbp, respectively, indicating the correct functioning of the electrophoresis, imaging, and analysis methods.

These chromosomes also provide a population of known sizes and relative numbers of molecules for testing whether this approach provides correct DSB frequencies in megabase pair-sized molecules. The sum of the lengths of the *H. wingei* chromosomal DNA (14.07 Mbp) is the length of this virtually ligated supermolecule, which we can consider as the untreated molecule that was treated to produce six breaks resulting in seven chromosomes. A dispersion curve was constructed based on the migration distance and lengths of the chromosomes of all three yeast species. The heavy bar in Figure 3 shows the extent of the *H. wingei* profile that was included in computing the $\bar{L}$ of the entire genome, yielding a value of 2.02 Mbp, in good agreement with the theoretical value of 2.01 obtained by dividing 14.07 Mbp by seven. The inverse of the calculated average length is thus 0.495 Mbp^{-1}, and since the inverse of the average length for the entire genome is 0.071, the yield of breaks per Mbp was 0.424. Multiplying by 14.07 Mbp/genome gives 5.97 breaks/genome, in excellent agreement with the actual number of six. This result clearly indicates the validity of the electrophoretic, imaging, and methods of moments analysis approaches in calculating number average lengths and break frequencies even in Mbp-size populations containing overlapping molecules that are poorly resolved by CHEF.

Transverse alternating field electrophoresis is an alternate pulsed field procedure. During electrophoresis, the DNA molecules execute a zigzag path downwards and from the front to the back of the vertically oriented gel (*28*). It can give excellent resolution of DNAs in the 1 Mbp range and provides a high sensitivity method for measuring double strand breaks in the ~1.3 Mbp family of human DNA fragments resulting from NotI digestion of genomic DNA (*5*). Figure 4 shows an electronic image of two lanes of a TAFE gel, containing λ ladders (lane 1), and in lane 2, the 15 *S. cerevisiae* chromosomes that enter the gel using this pulsing mode (the 2.2 Mbp chromosome does not enter the gel under these conditions). Figure 4 also shows the profiles of the fluorescence of ethidium bound to DNA in these two lanes and the dispersion curve derived from these two sets of DNAs. To test the dispersion function and migration of the DNAs according to molecular length, we determined the average lengths of each of the *S. cerevisiae* chromosomes, based on the profiles corresponding to each peak, using the dispersion function shown in the figure. Figure 5 shows that the calculated lengths agree well with the actual lengths of the 15 chromosomes (the complement includes two unresolved chromosomes at 1125 kbp).

To test the accuracy of calculation of the frequency of double strand breaks in DNAs dispersed by TAFE and quantified by number average length analysis, we used two portions of the *S. cerevisiae* profile shown in Figure 4. We first used the entire distribution (the region delimited by the heavy bar under the profile) and determined the break frequency using eq 5. For one gel, the $\bar{L}$ of the entire distribution was 759.4 kbp, in good agreement with the theoretical value of 757 kbp, obtained by dividing the length of the virtually ligated *S. cerevisiae* supermolecule (11 355 kbp for the chromosomes 1600 kbp and smaller that enter the gel and are dispersed by this TAFE regime) by 15. Using this sum of the lengths of the chromosomes as the untreated population, the break frequency was 13.95 breaks per genome, in excellent agreement with the actual value of 14 breaks required to generate the 15 chromosomes in the distribution on the gel from the virtually ligated supermolecule. Analysis of another TAFE gel, carried out one year later from entirely independent samples, also yielded 13.95 breaks/genome.

Double Strand Break Frequency Analysis in DNAs in the 1 Mbp-Size Region. A critical region of the DNA distribution is that in the ~1 Mbp region, which is used in high sensitivity quantitation of double strand breaks and clustered damages converted to double strand breaks in NotI-digested human DNA (*5*, *7*). We selected a portion of the distribution containing four chromosomes in this size region (1.125 Mbp doublet, 1.020 Mbp, and 0.945 Mbp, the sum of whose lengths is 4.215 Mbp) and selected the portion of the DNA profile shown by the broken line in Figure 4. Number average analysis of this region gave a number average length of 1.082 Mbp (cf. the theoretical value of 1.053); computation of the number of breaks required to convert the 4.215 Mbp virtually ligated supermolecule into the four chromosomes gave 2.89, in good agreement with the actual figure of 3.

Break Frequencies Computed from Independent DNA Length Standards. In the CHEF and TAFE analyses above, the experimental DNAs were among the length standards used to construct the dispersion curve for number average length analysis. Their inclusion makes the dispersion curve more robust. However, as long as the length standard DNAs span the size of the experimental DNAs and there are sufficient length standards for calculation of an adequate dispersion curve, number average length calculations should be valid when based on only independent DNA length standards (as it was for single-stranded DNAs (*6*)).

We validated the use of independent length standards in number average length analysis using two systems. First, the

DNA lengths and break (restriction site) frequencies for T7 and its restriction fragments shown in Figures 1 and 6 were obtained by use of independent DNA length standards (λ, HindIII digest of λ, and 100 bp ladder). Both the calculated length and the break frequencies correspond well to the actual values of known restriction sites.

Second, we tested the use of independent DNA length standards by calculating the frequency of breaks of the *H. wingei* virtually ligated supermolecule required to give the seven chromosomes (see Figures 3 and 6), excluding the *H. wingei* chromosomes in constructing the dispersion curve. The *S. pombe* and *S. cerevisiae* chromosomes span the entire range of the *H. wingei* chromosomal complement, and we used only their DNAs in constructing a dispersion curve. Because of the lack of markers in the intermediate size range (that of the *H. wingei* chromosomes), this dispersion curve is somewhat less robust than that based on all three species. Nevertheless, using the dispersion curve based only on *S. pombe* and *S. cerevisiae*, the number average length of the entire *H. wingei* complement was calculated to be 2091 kbp (cf. the theoretical value of 2010), corresponding to a value of 5.73 breaks/genome, still in reasonable agreement with the actual number of six.

Quantifying Double Strand Breaks and Oxidized Purine Clusters in T7 DNA. Since number average length analysis does not require specific distributions of breaks, it is equally applicable to DNA populations with random or other distributions of breaks as to those with specific sites as in the above analyses, for example, those induced by ionizing radiation. Such radiation induces complex damages in DNA—two or more strand breaks, oxidized bases, or abasic sites on opposing strands within a few helical turns. Double strand breaks (two or more closely opposed single strand breaks within a few helical turns) can be quantified directly by number average length analysis. In addition, other complex damages can be converted to de novo double strand breaks through action of enzymes recognizing their constituent lesions and then quantified by the same approach. Figure 7 presents such an analysis.

Figure 7A shows an electronic image of a neutral agarose gel containing X-irradiated (lanes 1−10) and γ-irradiated (lanes 11−20) T7 DNA, plus three sets of molecular length standards (M1, M2, and M3). DNAs in even-numbered lanes were treated with *E. coli* Fpg protein to measure oxidized purine clusters (*7*) (two or more lesions on opposing strands within a few helical turns, where at least one lesion is cleaved by Fpg protein, whose principal substrates are oxidized purines (*18*−*22*)). Figure 7B shows the profile of ethidium-bound DNA fluorescence in length standard lane M2 and the dispersion curve calculated from the length versus mobility relation of each standard. The lane profiles of two DNA samples [irradiated with 50 Gy X-ray, without (upper) and with (lower) treatment with Fpg protein] are shown as inserts. The extents of each experimental DNA profile correspond to the positions at which the fluorescence of DNA-bound ethidium bromide can be seen clearly and are shown by the horizontal bar in each profile in the insert. Table 1 contains the numerical results of such analyses. Figure 7C,D show a comparison of the results from this gel with those obtained previously for γ-ray induced DSB and oxidized purine clusters, respectively. The data from this gel for γ-ray induced DSBs (Figure 7C) are shown as large solid

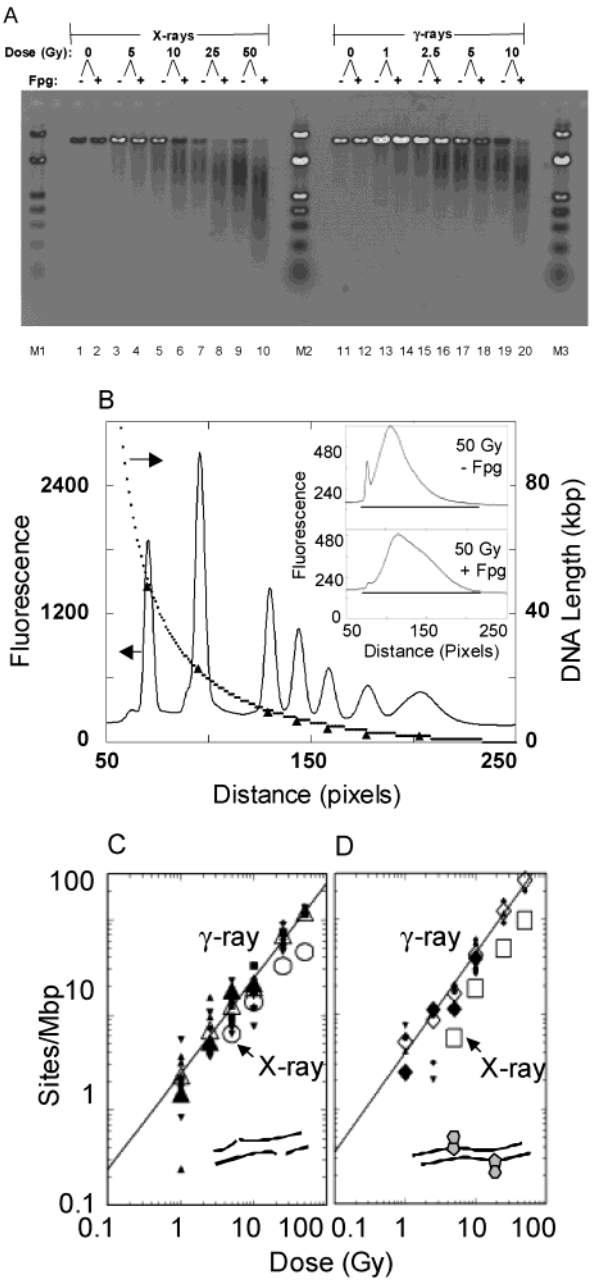

FIGURE 7: Number average length analysis of radiation-induced DNA double strand breaks and OxyPurine clustered damages. (A) Electronic image of electrophoretic gel showing T7 DNA exposed to increasing doses of X-rays (lanes 1−10) or γ-rays (lanes 11−20), then electrophoresed with (+Fpg) or without (−Fpg) treatment with Fpg protein, and three lanes of molecular length standard DNAs (M1, M2, M3). (B) DNA profile of lane M2 and the resulting dispersion curve. Insert, profiles of DNA irradiated with 50 Gy of X-rays, without (upper, corresponds to lane 9) and with (lower, lane 10) Fpg treatment. Horizontal bars show the portion of the profiles included in number average length analysis. (C) Quantitative data for double strand break induction from the gel in panel A, as compared to previous results for γ-irradiated DNA (*7*); small closed symbols, previous individual measurements; △, previous averages; ▲, current γ-ray DSB data; ○, current X-ray DSB data. (D) Oxypurine cluster yields. Small closed symbols, previous individual measurements; ◇, previous averages; ♦, current γ-ray OxyPurine cluster data; □, current X-ray cluster data.

triangles and are in the same range as previous individual measurements (small closed symbols) and averages of those data (open triangles) (*7*). The frequencies of OxyPurine clusters (Figure 7D) derived from this gel are shown as

Table 1: Analysis of DSBs and Damage Clusters by Number Average Length Analysis[a]

lane	dose (Gy)	Fpg treatment	$\bar{L}$ (bp)	DSB/Mbp	OxyPur clusters/Mbp
1	0	−	39 327		
2	0	+	37 295		1.39
3	5	−	31 501	6.32	
4	5	+	26 799		5.57
5	10	−	25 613	13.62	
6	10	+	17 408		18.4
7	25	−	17 239	32.58	
8	25	+	9353		48.91
9	50	−	14 045	45.77	
10	50	+	5956		96.71
11	0	−	37 010		
12	0	+	36 853		0.11
13	1	−	35 069	1.49	
14	1	+	32 209		2.53
15	2.5	−	31 048	5.19	
16	2.5	+	23 031		11.21
17	5	−	22 168	18.09	
18	5	+	17 674		11.47
19	10	−	20 634	21.44	
20	10	+	11 454		38.84

[a] The values of $\bar{L}$ computed by eq 5 are reported to the nearest base pair because this provides a precise estimate of the average molecular length for a given population. This does not, however, indicate that any of the electrophoretic modes used to obtain the data reported herein are capable of resolving large DNAs with single base accuracy. The resolving power achievable by static field gel electrophoresis has been discussed elsewhere (*32*). A similar exploration of the resolving power for UPFE, CHEF, and TAFE is being prepared (J. Sutherland, manuscript in preparation).

closed diamonds and are in the same range as the previous individual data (small closed symbols) and averages (open diamonds) (*7*). The yields of DSBs and clusters produced by 50 kVp X-rays appear to be lower, but this could be the result of attenuation of these low energy photons in the plastic and water of the tube used for irradiation.

DISCUSSION

Number average length analysis of breaks offers the potential of measurement of DNA damages in nanogram quantities of nonradioactive genomic DNA at damage levels as low as a few per gigabase pair. Furthermore, since there is no requirement in the underlying theory for any specific distribution of (damage) sites, it is a powerful method allowing analysis of breaks induced by quite different agents.

Quantification of breaks by number average length analysis and the use of a method of separating DNA molecules such as gel electrophoresis requires a known, unique migration versus length relationship, and second, accurate measurement of DNA masses on the gel. The criterion of DNA separation requires monotonic DNA migration, and each migration position must correspond to a single mean DNA size. In some pulsed field gel modes (e.g., field inversion), a single distance of migration may correspond to the mean position of migration of more than one size of DNA (*29*, *30*). Such modes do not fulfill the criterion demanded by number average length analysis and may not yield accurate number average lengths or break frequencies.

The second condition requires uniform and accurate measurement of the mass of DNA molecules at each position on the gel. This requires both quantitative biochemistry and electrophoresis (level gel of uniform composition, uniform fluorophore staining, adequate and uniform destaining, absence of migration-altering substances in the samples, and DNAs of linear configuration) as well as quantitative electronic imaging (uniform illumination of the gel, flat field optics, fluorescence intensities within the range of the detector) (*4*).

Double Strand Break Yield Assessment. Methods of calculating DNA damage frequencies are often evaluated by comparing results obtained with the method with those obtained by previously validated methods. Previously, we validated number average length analysis of DNAs dispersed by alkaline gel electrophoresis by comparing cyclobutyl pyrimidine dimer yields obtained by that method on DNA from UV-irradiated human cells with those obtained by dispersing the same DNAs by alkaline sucrose sedimentation (*6*), a gold standard of UV damage quantitation. However, for ionizing radiation, the available methods differ significantly in the yields of damages in genomic DNA per radiation dose (*31*). Thus, it is not clear which method is the gold standard for comparison. Some of this variability could reflect actual differences in yields because of experimental conditions (*9*, *10*), for example, presence of cellular radioquenchers, difference in chromosome length, or concomitant lesion repair during or immediately after irradiation.

The use of absolute DNA size standards and DNA populations with intact parental molecules and known numbers of daughter molecules (and thus of known numbers of breaks required to produce the daughter molecules) allows evaluation of the accuracy of calculation and break frequencies (as well as DNA lengths). We used this approach to test the validity of number average length analysis of electronic images of ethidium bromide-stained DNA populations in the size range of 4 kbp to 3 Mbp dispersed on electrophoretic gels, under the specific conditions of electrophoresis, imaging, and analysis described in Experimental Procedures and discussed above.

We first tested the relation of DNA migration versus length (DNA dispersion) for three specific pulsing regimes of UPFE, CHEF, and TAFE. Inspection of the dispersion curves in Figure 2 (UPFE), Figure 3 (CHEF), and Figure 4 (TAFE) indicates that the distribution of all the length standard molecules is single-valued, so the resulting dispersion functions can be represented by smooth monotonic curves. Further, a plot of the calculated lengths of DNAs of known sizes shows excellent one-to-one correspondence with their actual lengths (Figure 5). Because of the density of data points in the high molecular length region, to improve visibility, all the data points for *S. cerevisiae* chromosomes separated by CHEF Mode 2 were multiplied by 10, and those for multimers of λ separated by the same mode were divided by 100. Data for calculated DNA lengths in the size ranges best resolved by these gels (4−40 kbp for UPFE; ∼50 kbp to ∼1.5 Mbp for TAFE and ∼50 kbp to almost 6 Mbp for CHEF) are in excellent agreement with the one-to-one correspondence line relating the calculated number average lengths and actual DNA sizes.

The validity of the length determination functions provides a critical part of the total calculation of break levels. The use of DNA populations of known total length and known number of constituent components allows evaluation of the overall number average length analysis procedure. Figure 6 shows that the calculated break frequencies are in excellent

agreement with the actual numbers of breaks required to convert the parental molecule to its constituent daughters, whether restriction fragments or chromosomes. Furthermore, the correspondence holds for DNA molecules ranging from a few kbp to several Mbp.

An independent line of evidence also supports the validity of average length analysis for the quantification of double strand breaks. Instead of separating DNA molecules as a function of their size prior to measurement of fluorescence, the sizes were determined from the intensity of fluorescence emitted as they pass through a laser beam (*14*). Frequencies of γ-ray induced DSBs in T7 DNA determined using this procedure agree with yields determined by gel electrophoresis and method of moments calculation of number average lengths. These results demonstrate the validity of this gel electrophoresis/electronic imaging/method of moments/number average length analysis in strand break quantitation in DNA. The analysis and quantitative results of Figure 7 show that double strand breaks and clustered damages can readily be quantified by this approach. Of course, the sensitivity of number average length analysis depends on the size of the DNA molecule being analyzed. For molecules in the range of 50 kbp, damage levels from about one to about 100 sites per megabase pair can be easily measured using our biochemical, imaging, and analysis techniques. For larger molecules, the sensitivity increases accordingly. Thus, number average length analysis provides a versatile and accurate approach for quantifying DNA damages.

ACKNOWLEDGMENT

We thank Drs. Helen Evans and Nancy Olenick (Case Western Reserve University) and Dr. Raymond Warters (University of Utah) for critical reading of the manuscript.

REFERENCES

1. Cantor, C. R., and Schimmel, P. R. (1980) *Biophysical Chemistry*, W. H. Freeman & Co., New York.
2. Sutherland, J. C., Lin, B., Monteleone, D. C., Mugavero, J., Sutherland, B. M., and Trunk, J. (1987) *Anal. Biochem. 163*, 446−457.
3. Sutherland, J. C. (1990) in *Noninvasive Techniques in Biology and Medicine* (Freeman, S. E., Fukishima, E., and Green, E. R., Eds.) pp 125−134, San Francisco Press, San Francisco.
4. Sutherland, J. C., Monteleone, D. C., Trunk, J. G., Bennett, P. V., and Sutherland, B. M. (2001) *Electrophoresis 22*, 843−854.
5. Sutherland, B. M., Bennett, P. V., and Sutherland, J. C. (1996) *Anal. Biochem. 239*, 53−60.
6. Freeman, S. E., Blackett, A. D., Monteleone, D. C., Setlow, R. B., Sutherland, B. M., and Sutherland, J. C. (1986) *Anal. Biochem. 158*, 119−129.
7. Sutherland, B. M., Bennett, P. V., Sidorkina, O., and Laval, J. (2000) *Proc. Natl. Acad. Sci. U.S.A. 97*, 103−108.
8. Chen, C.-Z., and Sutherland, J. C. (1989) *Electrophoresis 10*, 318−326.
9. Warters, R. L., Newton, G. L., Olive, P. L., and Fahey, R. C. (1999) *Radiat. Res. 151*, 354−362.
10. Cedervall, B. E., and McMillan, T. J. (2002) *Radiat. Res. 158*, 247−249.
11. Sutherland, B. M., Bennett, P. V., Sutherland, J. C., and Laval, J. (2002) *Radiat. Res. 157*, 611−616.
12. Gulston, M., Fulford, J., Jenner, T., de Lara, C., and O'Neill, P. (2002) *Nucleic Acids Res. 30*, 3464−3472.
13. Sutherland, B. M., Harber, L. C., and Kochevar, I. E. (1980) *Cancer Res. 40*, 3181−3185.
14. Filippova, E. M., Monteleone, D. C., Trunk, J. G., Sutherland, B. M., Quake, S. R., and Sutherland, J. C. (2002) *Biophys. J. 84*, 1281−1290.
15. Doggett, N. A., Smith, C. L., and Cantor, C. R. (1992) *Nucleic Acids Res. 20*, 859−864.
16. Sutherland, J. C., Monteleone, D. C., Mugavero, J. H., and Trunk, J. (1987) *Anal. Biochem. 162*, 511−520.
17. Gardiner, K., Laas, W., and Patterson, D. (1986) *Somatic Cell Mol. Genet. 12*, 185−195.
18. Boiteux, S., O'Conner, T. R., Lederer, F., Gouvette, A., and Laval, J. (1990) *J. Biol. Chem. 265*, 3916−3922.
19. Boiteux, S., Gajewski, E., Laval, J., and Dizdaroglu, M. (1992) *Biochemistry 31*, 106−110.
20. Tchou, J., Kasai, H., Shibutani, S., Chung, M.-H., Laval, J., Grollman, A. P., and Nishimura, S. (1991) *Proc. Natl. Acad. Sci. U.S.A. 88*, 4690−4694.
21. Hatahet, A., Kow, W. Y., Purmal, A. A., Cunningham, R. P., and Wallace, S. S. (1994) *J. Biol. Chem. 269*, 18814−18820.
22. Jurado, J., Saparbaev, M., Matray, T. J., Greenberg, M. M., and Laval, J. (1998) *Biochemistry 37*, 7757−7763.
23. Karakaya, A., Jaruga, P., Bohr, V. A., Grollman A. P., and Dizdaroglu, M. (1997) *Nucleic Acids Res. 25*, 474−479.
24. Senturker, S., Bauche, C., Laval, J., and Dizdaroglu, M. (1999) *Biochemistry 38*, 9435−9439.
25. Sutherland, B. M., Bennett, P. V., Sidorkina, O., and Laval, J. (2000) *Biochemistry 39*, 8026−8031.
26. Dunn, J. J., and Studier, F. W. (1983) *J. Mol. Biol. 166*, 477−535.
27. Chu, G., Vollrath, D., and Davis, R. W. (1986) *Science 234*, 1582−1585.
28. Gardiner, K. (1991) *Anal. Chem. 63*, 658−665.
29. Carle, G. F., Frank, M., and Olson, M. V. (1986) *Science 232*, 65−68.
30. Gunderson, K., and Chu, G. (1991) *Mol. Cell Biol. 11*, 3348−3354.
31. Ward, J. F. (1990) *Int. J. Radiat. Biol. 57*, 1141−1150.
32. Ribeiro, E. A., and Sutherland, J. C. (1993) *Anal. Biochem. 210*, 378−388.

BI0205505